UDK 669.245:57.012.3
Original scientific article/Izvirni znanstveni članek

ISSN 1580-2949
Mater. Tehnol.

ANISOTROPIC MICROSTRUCTURAL EVOLUTION OF (001), (110) AND (111) PLANES IN SRR99 SINGLE-CRYSTAL SUPERALLOY

ANIZOTROPNI RAZVOJ MIKROSTRUKTURE NA RAVNINAH (001), (110) IN (111) V MONOKRISTALNI SUPERZLITINI TIPA SRR99

Xiaoli Zhang[1,a], Kuan Lei[1,a], Tingzhen Xin[1], Yishan Wu[2], Guiqun Liu[1*]

[1]College of Material Science and Engineering, North Minzu University, Ningxia, Yinchuan 750021, China
[2]Ningxia Coal Industry Co., Ltd., Yinchuan 750011, China
[a]These authors contributed equally to this work

Prejem rokopisa – received: 2025-07-11; sprejem za objavo – accepted for publication: 2025-10-10

doi:10.17222/mit.2025.1522

We investigate plane-dependent microstructures in an SRR99 single-crystal superalloy in the as-cast condition. Using optical and scanning electron microscopy, we examine sections parallel to the (001), (110), and (111) planes. Dendrite traces display "+" symmetry on (001), asymmetric "+" symmetry on (110), and an "×" pattern on (111). The γ' precipitates appear as irregular cube-like, triangular-prism-like, and triangular-pyramid-like shapes on (001), (110), and (111), respectively, whereas eutectic pools and carbides show no marked plane-dependent differences under the present conditions. These plane-specific observations provide a concise basis – limited to the as-cast state – for discussing anisotropic microstructural features that may be relevant to hot-cracking susceptibility and for clarifying how sectioning orientation influences apparent morphology in single-crystal superalloys.

Keywords: single-crystal superalloy, γ phase, γ' phase, dendrite morphology, eutectic, carbide

Avtorji v članku opisujejo raziskavo odvisnosti mikrostrukture od kristalografskih ravnin v liti monokristalni superzlitini vrste SRR99. V tej raziskavi so avtorji preiskovali preseke vzporedne ravninam (001), (110) in (111) s pomočjo vrstičnega elektronskega mikroskopa. Sledovi dendritov so kazali "+" simetrijo na ravnini (001), asimetrijo "+" na ravnini (110) in vzorec "×" na ravnini (111). Izločki γ' faze se pojavljajo kot nepravilna kubična, trikotna prizma in trikotna piramida na ravninah (001), (110) in (111). Pri tem evtektični »bazenčki« (meddendritni prostori) in karbidi v teh stanjih ne kažejo nobenih pomembnih razlik, odvisnih od kristalografskih ravnin. Opisana od ravnin odvisna specifična stanja lite mikrostrukture superzlitine omogočajo osnovno razlago njenih anizotropnih značilnosti, ki bi bile lahko pomembne za nastanek oziroma nagnjenost litine k tvorbi razpok v vročem in razjasnitev, kako orientacija sekcije kristalografskih ravnin vpliva na navidezno morfologijo v litih monokristalnih superzlitinah.

Ključne besede: monokristalna superzlitina v litem stanju (litina), fazi γ in γ', dendritna morfologija, evtektik, karbidi

1 INTRODUCTION

Superalloys exhibit excellent corrosion resistance and high-temperature performance, enabling them to operate above 600 °C while withstanding considerable stress. Based on their composition, superalloys can be categorized into iron-based, cobalt-based, and nickel-based superalloys. Nickel-based superalloys account for approximately 40 % of the market share and offer the best performance, making them widely used in the aerospace industry, e.g., for aeroengines and missiles.[1]

Nickel-based single crystal (SC) superalloys are typically produced using directional solidification techniques. These techniques involve creating a unidirectional temperature gradient between the solidified material and the unsolidified molten material. The crystal growth direction must be parallel and opposite to the heat-flow direction. Thus, the molten material solidifies along with the unidirectional temperature gradient. During the solidification process, the latent heat of crystallization increases the temperature of the solid-liquid interface. This leads to a negative temperature gradient and a supercooled state in the liquid phase. In this case, the solid-liquid interface tends to be non-flat. As a result, numerous dendrites begin to grow, with secondary dendrites branching from the primary ones. Until now the dendrite structures have been extensively studied and have been shown to play a crucial role in the material properties.[2–4]

SC materials are known for their anisotropy. For nickel-based SC superalloys with a face-centered cubic (FCC) crystal structure, the [001] direction is the fastest-growing and highest-performance direction. During the production of nickel-based SC superalloys, primary dendrites typically grow along the [001] direction.[5–8] Therefore, numerous studies have been conducted on the structure and properties along the [001] crystal orientation.

*Corresponding author's e-mail:
gqliu10b@alum.imr.ac.cn (Guiqun Liu)

So far, few studies have been conducted on different crystal planes of nickel-based SC superalloys. In this study, three different crystal planes were cut from the SRR99 SC superalloy. In addition, (001), (110) and (111) crystal plane samples were cut with a precision wire cutting machine. The findings related to dendrite morphologies, γ' phase morphologies, eutectic structure, and carbide content are presented herein.

2 EXPERIMENTAL MATERIALS AND METHODS

The SRR99 nickel-based single crystal (SC) superalloy used in this experiment is a first-generation material. The nominal composition of SRR99 is shown in **Table 1**.

Table 1: Nominal compositions of SRR99 alloy (*w*/%)

Cr	Co	W	Al	Ti	Ta	C	Ni
8.4	5.0	9.5	5.5	2.1	2.8	0.015	Bal.

Two methods are used to produce SC superalloys: the seeding method and the spiral selection method. The spiral selection method is efficient for producing SC superalloys but cannot accurately control the orientation of the crystal. The seeding method allows precise control of crystal orientation. Thus, the seeding method was selected to produce the SRR99 nickel-based SC superalloy in this experiment.

To define the section geometry, the following steps were taken. The (110) section was obtained by rotating the reference (001) sample by 45° about an in-plane [110] axis. The (111) section was prepared by rotating (001) by ≈54.7° about an in-plane ⟨110⟩ axis followed by azimuthal alignment. Angles were stated between the normals to the planes unless otherwise noted.

In the seeding method, a seed with the desired orientation was placed at the bottom of a ceramic mold to prevent random grain nucleation. The ceramic mold containing the required seed was heated to 1550 °C. The SRR99 alloy was superheated to 1550 °C and held at this temperature for 5 min to homogenize the melt. The molten alloy was then poured into the preheated mold. After a holding time of 10 min, allowing the system to reach the thermal equilibrium, the mold was withdrawn at a constant speed of 6 mm/min. Once the mold cooled to room temperature, it was broken to obtain the SRR99 SC.

Three sets of crystal planes, (001), (110), and (111), were cut into cubes of (10 × 10 × 10) mm using wire electrical discharge machining (Suzhou Baoma Numerical Control Equipment Co. Ltd., BM400C-CT). Following the metallographic process, three sets of samples with different crystal planes were prepared. The corrosion solution consisted of 100 mL HCl + 5 mL H_2SO_4 + 20 g $CuSO_4$ + 100 mL H_2O. The dendrite structures of the three crystal planes were observed using an optical microscope (Zeiss, Axio vert. A1). To study the γ/γ' phase, carbide and eutectic structure, three different crystal planes were observed using a scanning electron microscope (Zeiss, Sigma500).

3 RESULTS AND DISCUSSION

3.1 Dendritic structure

Figure 1 shows the dendritic morphologies of three different crystal planes of SRR99 nickel-based SC superalloy. It was found that the dendritic morphologies of the three crystal planes were obviously different. As shown in the (001) crystal plane on **Figure 1a**, the dendrites are symmetrical "+", and their centers correspond to the primary axis along the [001] direction. The four symmetrical directions of the dendrites correspond to the secondary dendrite arms. The dendrites extending from the secondary arms are the tertiary dendrite arms. Due to the existence of the tertiary dendrite arms, the "+" shape of dendrites is less distinct. The (110) section was obtained by rotating the reference (001) sample by 45° about the in-plane [110] axis and using wire cutting. As shown in the (110) crystal plane on **Figure 1b**, the dendrites of the (110) crystal plane exhibit an asymmetric "+" shape. The two secondary dendrite arms along one direction are particularly long, while the two dendrite arms along the other direction are particularly short. As shown in the (111) crystal plane on **Figure 1c**, the dendritic morphology of the (111) crystal plane is symmetrical "×".

In **Figures 1a-b-c**, the black area between adjacent dendrites is the interdendritic region, and the bright white areas within the interdendrite are the eutectic[4].

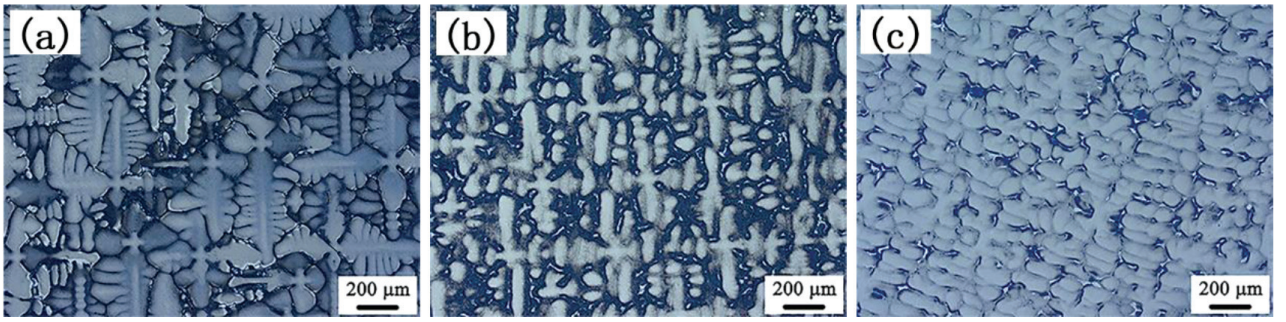

Figure 1: Dendritic structures of the three crystal planes at 50× magnification: a) (001) crystal plane; b) (110) crystal plane; c) (111) crystal plane

3.2 γ/γ'phase

As shown in **Figures 2** and **3**, the white gray grid area represents the γ phase matrix. The black sunken regions correspond to the γ' phase of the secondary precipitation. The γ' phase morphologies of the three crystal planes exhibited significant differences. The γ' phase of the (001) crystal plane appeared as an irregular cubic shape. Since the (110) sample was obtained by rotating the (001) sample by 45°, the γ' phase on the (110) crystal plane exhibited an irregular triangular prism shape. Similarly, since the (111) sample was obtained by rotating the (001) sample by 54.7°, the γ' phase on the (111) crystal plane exhibited an irregular triangular pyramid shape. The irregular γ' phases observed on the three crystal planes were attributed to the cast samples not being heat treated. If they had been subjected to heat treatment, the γ' phases would have been more regular.

A nickel-based SC superalloy typically consists of a γ phase with a disordered face-centered cubic crystal structure and γ' phase with an ordered face-centered cubic crystal structure ($L1_2$). The γ' phase is a crystal structure strengthened by solid solution elements.[9,10] Due to the strengthening γ' phase, a nickel-based SC superalloy exhibits excellent strength and creep resistance. The strength of the most materials decrease with increasing temperature, but the γ' phase shows the opposite temperature dependence in the process of uniaxial tension.[11–15] This phenomenon is attributed to the movement of superdislocations. The Burgers vector required for a fault in the γ' lattice to revert to its original state is twice that of a single dislocation in the γ phase.

Due to the energy barrier associated with planar fault formation, known as the anti-phase boundary (APB), dislocations in the γ' phase must move in pairs. The dislocations and their paired counterparts are referred to as superpartials and superdislocations, respectively. For instance, the resolved shear stress measured under uniaxial compression increased by more than a factor of four at the peak temperature of 1000 K compared to room temperature in Ni_3(Al, Nb).[13] This anomalous behavior was attributed to the thermally activated cross-slip of superdislocations from the {111} planes to the {100} planes with lower APB energy, which acted as a self-trapping mechanism known as Kear-Wilsdorf (KW) locks.[16–18] Consequently, the inverse temperature dependence of γ' strength is recognized as one of the key strengthening mechanisms for Ni-based superalloys.[10]

3.3 Eutectic structure

To frame the discussion, we treat the eutectic influence factor as a conceptual, qualitative index defined as $E = Ve \times Se$, where *Ve* denotes the apparent eutectic fraction (e.g., area fraction in micrographs) and *Se* denotes the characteristic size of eutectic pools (e.g., equivalent-circle diameter). All statements below are limited to the as-cast condition and visual inspection under comparable fields of view; rigorous plane-by-plane quantification is beyond the scope of this work.

During the process of directional solidification, dendritic trunks solidified first and interdendritic regions solidified later. For the solidification of the as-cast SRR99 nickel-based SC superalloy, the formation of eutectic oc-

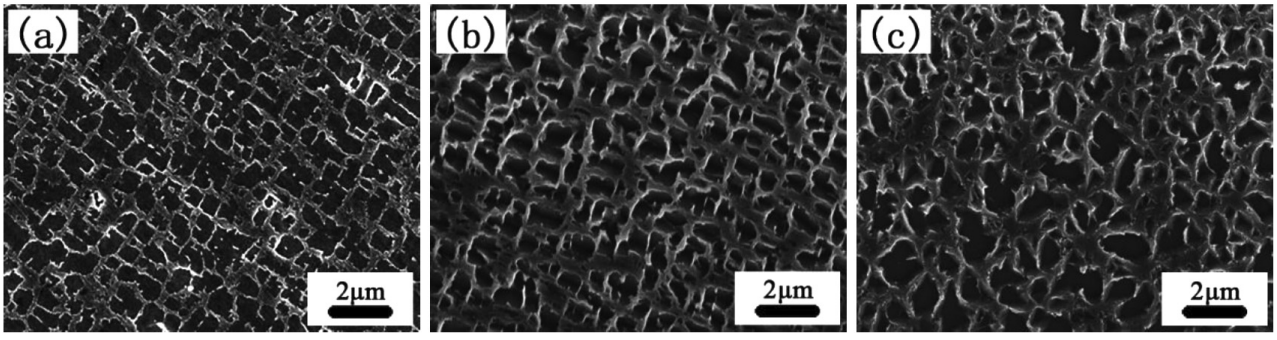

Figure 2: γ/γ' phases of the three crystal planes at 10000× magnification: a) (001) crystal plane; b) (110) crystal plane; c) (111) crystal plane

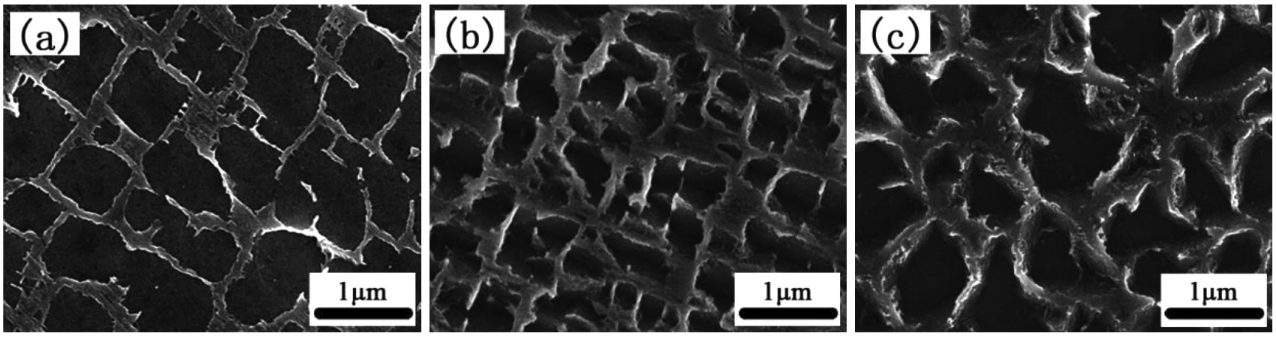

Figure 3: γ/γ' phases of the three crystal planes at 30000× magnification: a) (001) crystal plane; b) (110) crystal plane; c) (111) crystal plane

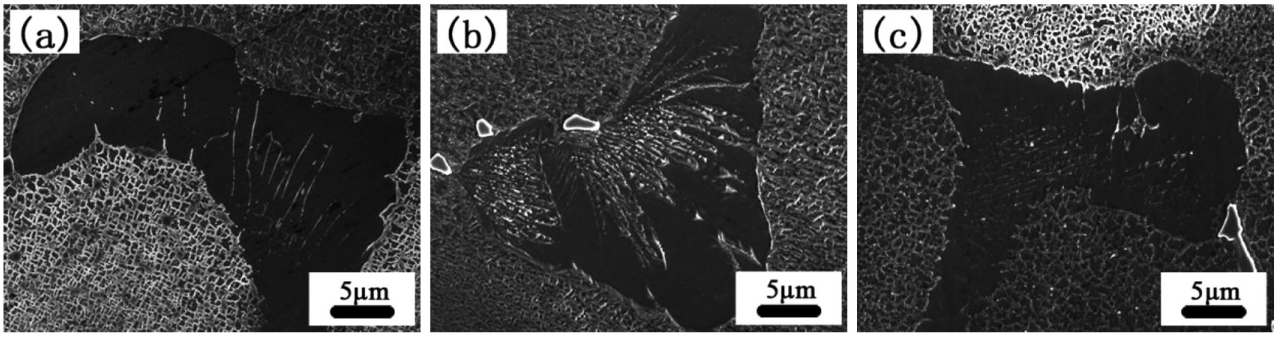

Figure 4: Eutectic structures of the three crystal planes at 4000× magnification: a) (001) crystal plane; b) (110) crystal plane; c) (111) crystal plane

curred later than that of dendritic trunks. The eutectic was formed from the co-crystallization of γ and γ' phases in the interdendritic regions. As shown in **Figure 4**, the eutectic structure was composed of a large quantity of the black γ' phase and a small amount of the white-gray γ phase.

There were no significant differences between the eutectic morphologies of the three crystal planes. The existence of the eutectic structure could reduce the stability of the alloy and lead to hot cracking. Thermal cracking sensitivity was closely related to eutectic characteristics. It occurred because eutectic characteristics reflected the solidification process, segregation behavior and coalescence behavior of dendrite. Apart from the other factors, the size and volume fraction of the γ/γ' eutectic structure were not sufficient to evaluate the effect of eutectic characteristics on hot cracking sensitivity.[19]

Therefore, we use the eutectic influence factor (E) as the qualitative index in the as-cast condition, defined as:

$$E = Se + Ve$$

where *Ve* denotes the apparent eutectic fraction (i.e., the area fraction in micrographs) and *Se* denotes the characteristic size of eutectic pools (e.g., equivalent circle diameter).

The E value is consistent with hot cracking sensitivity.[20] From our results (**Figure 1**), the volume fractions of eutectic of the (110) and (111) planes were larger than that of the (001) plane. Therefore, the influence of this factor on the hot cracking sensitivity of the (110) and (111) planes is higher than in the case of the (001) plane.

3.4 Carbides

Four types of carbide structures with distinct morphologies were observed, namely acicular, spherical, massive and Chinese character.[21] As shown in **Figure 5**, the carbide morphology of the three crystal planes exhibited the Chinese-character form.

The possible types of carbides in nickel-based SC superalloys are MC, M_6C and $M_{23}C_6$. According to the previous studies, different metal elements are enriched in different carbides. Ta and Ti are rich in the MC carbide. W is rich in the M_6C carbide. Furthermore, Cr is rich in the $M_{23}C_6$ carbide. In this experiment, the energy spectrum compositions of carbides were analyzed, as shown in **Figure 6**. The diffraction pattern analysis indicated that Ta and Ti were rich in carbide. Thus, the type of carbide was the MC carbide.

In the early nickel-based SC superalloys, carbon was not added, so carbides generally did not appear. However, with the development of technology and continuous change in the composition of alloy elements, the addition of carbon could lead to the formation of carbides. Carbide could strengthen the grain boundary. Thus, carbon was a grain-boundary strengthening element. The size and volume fraction of carbides increased with the increase in the carbon content.[20–25]

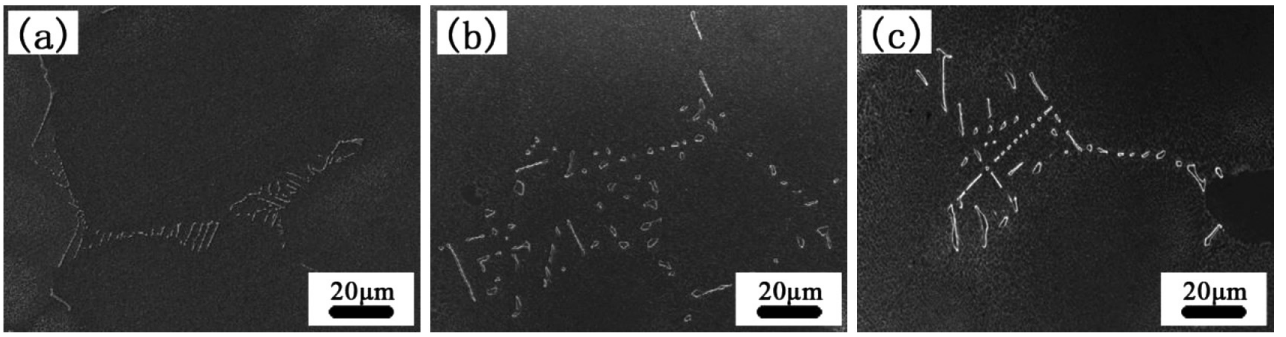

Figure 5: Carbide structures of the three crystal planes at 4000× magnification: a) (001) crystal plane; b) (110) crystal plane; c) (111) crystal plane

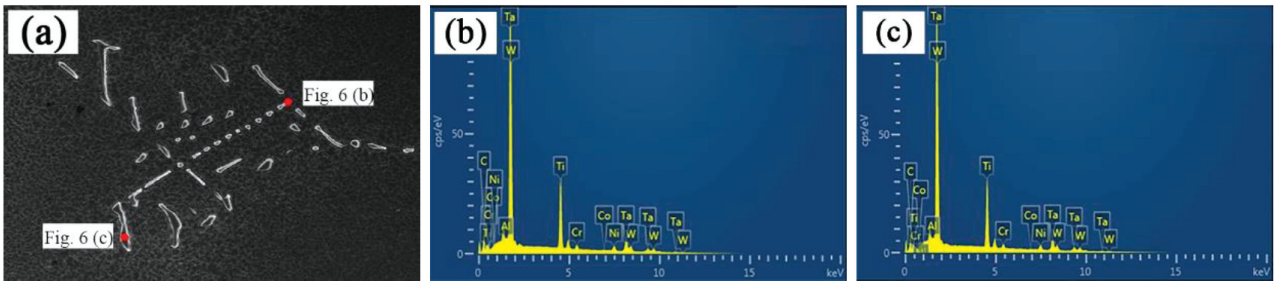

Figure 6: Composition energy spectra of the carbides: a) selected area diffraction patterns at their interface (SEM); b) map of selected area 1; c) map of selected area 2

4 CONCLUSIONS

In the as-cast condition, dendritic morphologies of the three planes were distinct: (001) exhibited "+" symmetry, (110) an asymmetric "+" pattern, and (111) an "×" pattern. The dendrites of the (001) crystal plane were symmetrical "+", the dendrites of the (110) crystal plane were asymmetric "+", and those of the (111) crystal plane were symmetrical "×".

The γ' phase morphologies of the three crystal planes were also significantly different. The γ' phase of the (001) crystal plane was an irregular cube, the γ' phase of the (110) crystal plane was an irregular triangular prism, and that of the (111) crystal plane was an irregular triangular pyramid.

Under the present as-cast, image-based observations, the eutectic morphology and carbide distribution did not show marked plane-dependent differences. Where referenced, the eutectic influence factor (E) was used only as a qualitative index to frame the discussion and did not imply a statistical ranking among the planes.

Acknowledgment

This work was supported by the Young Top-Notch Talents of Ningxia Province [2022033] and the Graduate Innovation Program of North Minzu University [YCX24301].

5 REFERENCE

[1] J. Zhang, L. Wang, G. Xie, D. Wang, J. Shen, Y. Lu, Y. Huang, Y. Li, Recent Progress in Research and Development of Nickel-Based Single Crystal Superalloys, Acta Metall. Sin., 59 (**2023**) 9, 1109–1124, doi:10.11900/0412.1961.2023.00140

[2] X. Zhang, L. Feng, Y. Yang, Y. Zhou, G. Liu, Influence of Secondary Orientation on Competitive Grain Growth of Nickel-Based Superalloys, Acta Metall. Sin., 56 (**2020**) 7, 969–978, doi:10.11900/0412.1961.2019.00396

[3] X. Zhang, Y. Yang, G. Liu, et al., Primary Dendrite Spacing in Single Crystal Superalloy Prepared by Directional Solidification, Foundry Technol., 39 (**2018**) 1, 21–24, doi:10.16410/j.issn1000-8365.2018.01.005

[4] X. Zhang, T. Xin, S. Yue, X. Meng, G. Liu, Statistical study of the primary-dendrite spacings in single-crystal superalloys, Mater. Tehnol., 55 (**2021**) 1, 149–153, doi:10.17222/mit.2020.161

[5] C. Li, C. Wei, R. L. Zhang, et al., Effects of directional solidification parameters and crystal selector on microstructure of single crystal of Ni-base superalloys, J. Cent. South Univ., 25 (**2018**) 1, 1–8, doi:10.1007/s11771-018-3711-1

[6] S. Zhang, S. Tian, H. Yu, L. Yu, X. Yu, Microstructure evolution and FEM analysis of [111] oriented single crystal of a nickel-based superalloy during tensile creep, Acta Metall. Sin., 48 (**2012**) 5, 561–568, doi:10.3724/SP.J.1037.2011.00536

[7] G. A. Chadwick, Directionally Solidified Materials for High Temperature Service, Br. Corros. J., 19 (**2013**) 4, 154–155, doi:10.1179/000705984798273164

[8] M. Xu, X. Zhang, X. Geng, G. Liu, Y. Wang, Z. Wang, J. Guo, Microstructure Characterization and Competitive Crystal Growth of Directional Solidified Nickel-based Single Crystal Superalloy during Spiral Grain Selector, Spec. Cast. Nonferrous Alloys, 41 (**2021**) 7, 831–836, doi:10.15980/j.tzzz.2021.07.008

[9] P. C. Gasson, The Superalloys: Fundamentals and Applications, Aeronaut. J., 112 (**2008**) 1131, 372–291, doi:10.1017/S0001924000087509

[10] J. Ruzic, K. Goto, I. Watanabe, T. Osada, L. Wu, T. Ohmura, Temperature-dependent deformation behavior of γ and γ' single-phase nickel-based superalloys, Mater. Sci. Eng. A, 818 (**2021**), 141439, doi:10.1016/j.msea.2021.141439

[11] S. Korte, R. J. Stearn, J. M. Wheeler, et al., High temperature microcompression and nanoindentation in vacuum, J. Mater. Res., 27 (**2012**) 1, 167–176, doi:10.1557/jmr.2011.268

[12] B. D. Beake, A. J. Harris, Nanomechanics to 1000 °C for high temperature mechanical properties of bulk materials and hard coatings, Vacuum, 159 (**2019**) 17–28, doi:10.1016/j.vacuum.2018.10.011

[13] D. P. Pope, S. S. Ezz, Mechanical properties of Ni_3Al and nickel-base alloys with high volume fraction of γ', Int. Mater. Rev., 29 (**1984**) 1, 136–167, doi:10.1179/imtr.1984.29.1.136

[14] X. S. Li, D. J. Smith, Temperature and orientation dependence of elastic and yield properties of single crystal nickel base superalloy, Mater. Sci. Technol., 11 (**1995**) 12, 1253–1260, doi:10.1179/mst.1995.11.12.1253

[15] S. Takeuchi, E. Kuramoto, Temperature and orientation dependence of the yield stress in Ni_3Ga single crystals, Acta Metall., 21 (**1973**) 4, 415–425, doi:10.1016/0001-6160(73)90198-3

[16] M. Demura, D. Golberg, T. Hirano, An athermal deformation model of the yield stress anomaly in Ni_3Al, Intermetallics, 15 (**2007**) 10, 1322–1331, doi: 10.1016/j.intermet.2007.04.007

[17] P. Veyssière, Yield stress anomalies in ordered alloys: a review of microstructural findings and related hypotheses, Mater. Sci. Eng. A, 309–310 (**2001**) 44–48, doi:10.1016/S0921-5093(00)01662-2

[18] G. R. Weber, S. Ghosh, Thermo-mechanical deformation evolution in polycrystalline Ni-based superalloys by a hierarchical crystal plasticity model, Mater. High Temp., 33 (**2016**) 4–5, 401–411, doi:10.1080/09603409.2016.1190147

[19] Y. Z. Zhou, A. Volek, Effect of dendrite arm spacing on castability of a directionally solidified nickel alloy, Scr. Mater., 56 (**2007**) 6, 537–540, doi:10.1016/j.scriptamat.2006.11.002

[20] Z. Zhao, J. X. Dong, Effect of Eutectic Characteristics on Hot Tearing of Cast Superalloys, J. Mater. Eng. Perform., 28 (**2019**) 8, 4707–4717, doi:10.1007/s11665-019-04230-9

[21] Z. Yu, L. Liu, J. Zhang, Effect of carbon addition on carbide morphology of single-crystal Ni-based superalloy, Trans. Nonferrous Met. Soc. China, 24 (**2014**) 2, 339–345, doi:10.1016/S1003-6326(14)63066-1

[22] L. R. Liu, T. Jin, N. R. Zhao, Z. H. Wang, X. F. Sun, H. R. Guan, Z. Q. Hu, Effect of carbon addition on the creep properties in a Ni-based single crystal superalloy, Mater. Sci. Eng. A, 385 (**2004**) 1–2, 105–112, doi:10.1016/j.msea.2004.06.003

[23] E. R. Cutler, A. J. Wasson, G. E. Fuchs, Effect of minor alloying additions on the carbide morphology in a single crystal Ni-base superalloy, Scr. Mater., 58 (**2008**) 2, 146–149, doi:10.1016/j.scriptamat.2007.09.050

[24] W. R. Sun, J. H. Lee, S. M. Seo, S. J. Choe, Z. Q. Hu, The eutectic characteristic of MC-type carbide precipitation in a DS nickel-base superalloy, Mater. Sci. Eng. A, 271 (**1999**) 1–2, 143–149, doi:10.1016/S0921-5093(99)00189-6

[25] E. Balikci, R. A. Mirshams, A. Raman, Fracture behavior of superalloy IN738LC with various precipitate microstructures, Mater. Sci. Eng. A, 265 (**1999**) 1–2, 50–62, doi:10.1016/S0921-5093(99)00012-X